ELSEVIER

Earth and Planetary Science Letters 163 (1998) 327–342

EPSL

Refining the eustatic sea-level curve since the Last Glacial Maximum using far- and intermediate-field sites

Kevin Fleming *, Paul Johnston, Dan Zwartz [1], Yusuke Yokoyama, Kurt Lambeck, John Chappell

Research School of Earth Sciences, Australian National University, Canberra, ACT, 0200, Australia

Received 18 June 1998; revised version received 27 August 1998; accepted 3 September 1998

Abstract

The eustatic component of relative sea-level change provides a measure of the amount of ice transferred between the continents and oceans during glacial cycles. This has been quantified for the period since the Last Glacial Maximum by correcting observed sea-level change for the glacio-hydro-isostatic contributions using realistic ice distribution and earth models. During the Last Glacial Maximum (LGM) the eustatic sea level was 125 ± 5 m lower than the present day, equivalent to a land-based ice volume of (4.6–4.9) $\times\ 10^7$ km^3. Evidence for a non-uniform rise in eustatic sea level from the LGM to the end of the deglaciation is examined. The initial rate of rise from ca. 21 to 17 ka was relatively slow with an average rate of ca. 6 m ka^{-1}, followed by an average rate of ca. 10 m ka^{-1} for the next 10 ka. Significant departures from these average rates may have occurred at the time of the Younger Dryas and possibly also around 14 ka. Most of the decay of the large ice sheets was completed by 7 ka, but 3–5 m of water has been added to the oceans since that time.

Keywords: eustacy; sea-level changes; last glacial maximum; Holocene

1. Introduction

Changes in sea level relative to its present position result from variations in the shape or volume of the oceans, the redistribution of water within the ocean basins, and the vertical movement of coastal areas. Driven by internal earth processes and the growth and decay of ice sheets, these changes have different characteristic time and length scales. For example, mantle dynamic processes alter global ocean basin shapes on time scales of 10^6 years and longer. Crustal and lithospheric tectonic processes introduce differential movements between land and sea on both short and long time scales but with much shorter characteristic length scales of the order of a few hundred kilometres or less. The sea-level change caused by glacial cycles has both a global and regional character but the predominant characteristic time scale is between 10^3 and 10^5 years. It is this last contribution that is discussed here, with particular emphasis on changes since the last maximum glaciation.

The aim of this paper is to provide improved constraints on the eustatic sea-level curve since the time of the Last Glacial Maximum (LGM). Over the

* Corresponding author. Tel.: +61 2 6249 5521; Fax: +61 2 6249 5443; E-mail: kevin@rses.anu.edu.au

[1] Present address: Institute for Marine and Atmospheric Research Utrecht, Utrecht University, Utrecht, the Netherlands.

PII: S0012-821X(98)00198-8

past 20000 years changes in ocean volume have been primarily caused by the melting of the major Late Pleistocene ice sheets and the eustatic sea-level curve provides a constraint on the changing land-based ice volumes during this time. This time-dependent eustatic function $\Delta\zeta_{esl}$ is defined as

$$\Delta\zeta_{esl}(\tau) = -\left(\frac{\rho_{ice}\Delta V_{ice}(\tau)}{\rho_{water}A_o(\tau)}\right) \quad (1)$$

where ρ_{ice} and ρ_{water} are the densities of ice and water respectively, ΔV_{ice} is the difference in the global, land based, ice volume between time τ and the present and A_o is the surface area of the ocean (e.g. [1]). $\Delta\zeta_{esl}$ therefore provides a measure of the change in ocean volume and, indirectly, of ice volume. This function provides not only one of the essential inputs into modelling glacial rebound and the associated consequences of spatially variable sea-level, gravity and earth rotation changes, but it can also provide a calibration of proxy sea-level indicators such as the $\delta^{18}O$ record from deep sea sediment cores.

The eustatic sea-level function provides a zero-order description of sea level change and the actual change can depart significantly from this because of tectonic and glacio-hydro-isostatic effects. The former can often be evaluated from independent evidence and in some circumstances can be corrected for (e.g. [2]), whereas the latter can be predicted from appropriate isostatic models. The isostatic corrections are largest within and near the ice sheets and the eustatic function is best estimated from sea-level data collected far from the former ice margins where the glacio-isostatic effects are smaller. The present analysis is largely restricted to such localities. Three intervals of the eustatic sea-level function will be emphasised. The first is its value during the LGM when sea levels at far-field sites were at their lowest. Eustatic values from this period constrain the volume of ice that had accumulated on the continents at this time, as well as the duration and timing of this glacial stage. The second is the rate of sea-level change during the Late Glacial Period (LGP), extending until about 7000 years ago. This part of the eustatic curve establishes the average rate at which the former ice sheets melted, as well as any variation in this rate during the interval. The third is the Post Glacial Period (PGP), extending from about 7000 years ago to the present. This interval is of interest for establishing whether changes in ocean volume occurred after most melting was completed, due to the slow but ongoing melting of the remaining glaciers of Antarctica, Greenland and mid-latitude glaciers.

Section 2 of this paper defines the components of glacio-hydro-isostatic sea-level change and their global pattern. Section 3 discusses the requisite model parameters, including the earth's rheology and the nominal ice distribution, as well as the calibration of the radiocarbon time-scale and the uncertainties in sea-level observations. Section 4 reviews the observational evidence used (Fig. 1); LGM data from around the world, LGP data from Barbados, Papua New Guinea and Tahiti, and PGP data from the Great Barrier Reef (Australia), the Senegal River (West Africa), Jamaica, and the west coast of Malaysia. The inferred eustatic function is interpreted in Section 5 and the conclusions are summarised in Section 6.

2. Ice sheets and sea-level change

2.1. Components of isostatic sea-level change

In the absence of tectonics, the change in relative sea level ($\Delta\zeta_{rsl}$) for time τ and location φ can be expressed schematically as (e.g. [3–5]):

$$\begin{aligned}\Delta\zeta_{rsl}(\tau,\varphi) &= \Delta\zeta_{esl}(\tau) + \Delta\zeta_{iso}(\tau,\varphi)\\ &= \Delta\zeta_{esl}(\tau) + \Delta\zeta_{ice}(\tau,\varphi) + \Delta\zeta_{water}(\tau,\varphi)\\ &\quad + \Delta\zeta_{rotation}(\tau,\varphi) \qquad (2)\end{aligned}$$

where $\Delta\zeta_{iso}$ is the total isostatic effect associated with the glacial rebound process and $\Delta\zeta_{ice}$ and $\Delta\zeta_{water}$ are the components of $\Delta\zeta_{iso}$ representing the combined ice (glacio-isostatic) and water (hydro-isostatic) load contributions. The theory that describes these terms is gravitationally consistent with mass conserved and sea level remaining an equipotential surface over the globe. The glacio-isostatic term includes the vertical movement of the earth's crust caused by changes in ice loading and the effect of changes to the earth's gravitational field due to the redistribution of the mass on and within the planet.

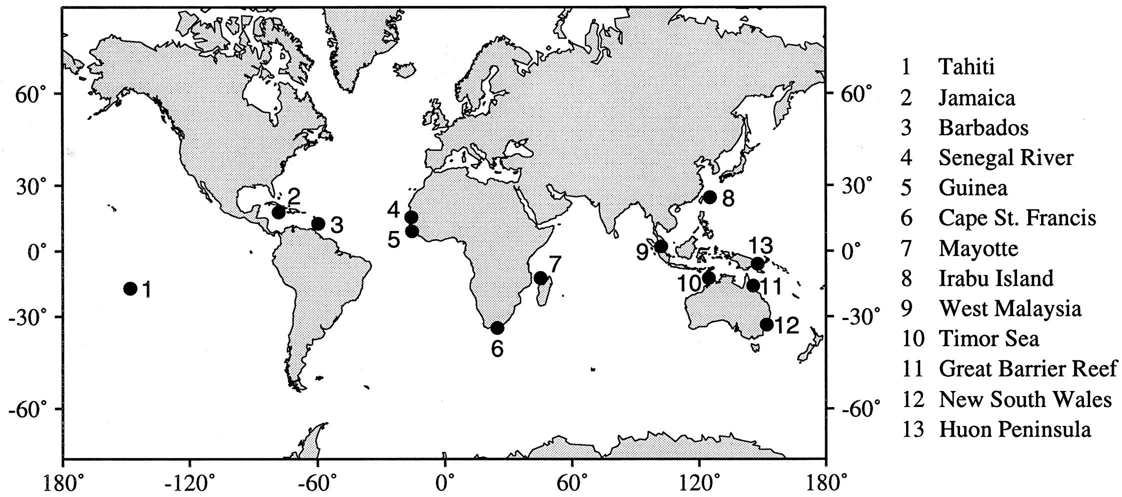

Fig. 1. Locality map for the sea-level sites discussed in this paper.

It is therefore a function of the spatial and temporal history of the global ice distribution and the earth's rheology. The hydro-isostatic term includes the crustal displacement and gravitational effects associated with the redistribution of ocean waters and is a function of the rheology, coastal geometry and eustatic sea level. A rigorous iterative procedure is used to calculate this term, which includes the modification of the ocean area as sea-level changes [5,6]. Solutions for $\Delta\zeta_{\mathrm{rsl}}$ converge to less than a few cm within four iterations. The redistribution of mass in the earth-ocean system also modifies the planet's inertia tensor, hence its rotation and centrifugal force, and the consequences this has on relative sea-level change are included in the last term, $\Delta\zeta_{\mathrm{rotation}}$ [7].

2.2. Geographical variation in sea-level change

Components of isostatic sea-level change vary with geographical location and it is this spatial variation that allows the earth's rheology and aspects of the history of past ice sheets to be inferred from sea-level observations [1,8]. For locations within the margins of the larger ice sheets at their maximum extent, referred to as near-field sites, the dominant isostatic term $\Delta\zeta_{\mathrm{ice}}$ is positive with relative sea levels during the LGP and PGP above the present day position, despite the increase in ocean volume that occurred during the same interval. Model predictions of this change are dependent on both the mantle rheology parameters and on details of the ice sheet geometry. Hence any estimates of the eustatic contribution from such observations would be strongly dependent on the model assumptions made and therefore such sites have been avoided in this analysis. For localities at intermediate distances beyond the limits of glaciation, the so-called intermediate-field sites, the glacio-isostatic contribution is much reduced in magnitude but it remains the dominant term. However, its sign is now mostly negative because the crust in this region is subsiding in response to the flow of mantle material towards the area of former glaciation. This zone typically extends for several thousand kilometres beyond the former ice margin [4]. In this region, the sea-level curve is characterised by a continually rising function from the time of the LGM to the present, with the rate of rise significantly slower during the PGP than the LGP. Because the isostatic terms are relatively small, isostatic predictions for sites within this zone are less dependent on details of the ice models than for near-field sites and observations from these localities would provide better constraints on the eustatic function. Of the sites considered in this paper, only Jamaica and possibly Barbados lie within this zone. Much further from the ice margins, at the far-field sites, the hydro-isostatic contribution usually dominates the glacio-isostatic signal, although the total isostatic correction is small and the sea level curve approximates the eustatic function. In particular, sea-level change during the

LGP is not strongly dependent on the choice of mantle rheology and is independent of details of the ice load geometry, but is dependent on the timing and rates of bulk melting of the ice sheets [8]. It is for these reasons that the emphasis of this paper is on observational evidence from far-field localities (see Fig. 1).

3. Model and data dependence

3.1. Earth rheology

The earth's rheology is described by a three-layer mantle model, consisting of an elastic lithosphere (effective lithosphere thickness $H_{\rm lith}$), an upper mantle from the base of the lithosphere down to 670 km, and a lower mantle down to the core-mantle boundary. The mantle response is defined as a Maxwell solid with effective upper and lower mantle Newtonian viscosities of $\eta_{\rm um}$ and $\eta_{\rm lm}$ respectively. Realistic depth profiles for density and elastic parameters are based on the PREM [9].

Analyses of glacial rebound and sea-level data from near-, intermediate- and far-field localities has provided some constraints to estimates of the mantle parameters, recent estimates for which are summarised in Table 1 (e.g. [1,10,11]). Some of this variability may come from lateral heterogeneity in the earth's rheology and some may represent uncertainty in the analyses. Fig. 2 illustrates predicted $\Delta\zeta_{\rm iso}$ for two sites, Barbados (intermediate- to far-field) and the Huon Peninsula (Papua New Guinea, far-field), as a function of rheology parameters that encompass the range of values in Table 1. At both locations $\Delta\zeta_{\rm iso}$ shows little dependence on $H_{\rm lith}$, the difference between extreme results being <1 m at the LGM for both sites. The dependence of $\Delta\zeta_{\rm iso}$ on viscosity is greater; the difference at 21 ka between the upper and lower limits indicated in Table 1 being ca. 3.5 m for $\eta_{\rm um}$ and ca. 5 m for $\eta_{\rm lm}$. By 7 ka the dependence these isostatic corrections has on both parameters has decreased to <1 m for both sites.

Table 1
Summary of the plausible upper and lower limits to the earth model parameters for a three-layer earth

Parameter	Lower limit	Upper limit
$H_{\rm lith}$ (km)	50	100
$\eta_{\rm um}$ ($\times 10^{20}$ Pa s)	2	6
$\eta_{\rm lm}$ ($\times 10^{21}$ Pa s)	5	20

3.2. Ice distribution

For far- and near-field sites, $\Delta\zeta_{\rm iso}$ is dependent primarily on the bulk characteristics of the ice load; the total volume of ice involved, the timing of the disintegration of the ice sheets and, to a lesser degree, on the details of ice distribution within the ice sheets. While the unloading cycle is most important, the choice of loading cycle is not insignificant. For example, a rapid build-up, with a short maximum period followed by a rapid disintegration results in relative sea-level curves that lag behind the corresponding eustatic change. The nominal ice distribution used in this paper (Fig. 3) is comprised of three parts; Antarctica, western Northern Hemisphere and the European ice sheets. The Antarctic ice model is the least well defined and is derived from the ANT3A model [8,12] with a $\Delta\zeta_{\rm esl}$, based on the present day ocean area, of ca. -27 m at the LGM (60% of the original) and 3 m melting since 7 ka. The western Northern Hemisphere (North America, Greenland and Iceland) is derived from the ARC3 model which in turn is based on the ICE-1 model [13,14]. The $\Delta\zeta_{\rm esl}$ at the LGM for this contribution is ca. -62 m with melting completed by 6.8 ka. The European ice model, made up of the Fennoscandian, British Isles and Barents and Kara Seas ice sheets, is also from the ARC3 model and has a LGM $\Delta\zeta_{\rm esl}$ of ca. -26 m, with melting completed by 8.8 ka [8,13,14]. This gives a total $\Delta\zeta_{\rm esl}$ of ca. -114 m for the change in global ice volume since the LGM. Contributions from mountain glaciers have been ignored. The eustatic curve before the LGM is based on the δ^{18}O signal from deep-sea sediment cores (e.g. [15]) and calibrated using the Huon Peninsula raised reef record [16]. These ice sheets are assumed to maintain the same ice geometry/eustatic sea level relationship before the LGM as after it.

3.3. Estimating the eustatic sea level

From Eq. 2, a correction term $\delta\zeta_{\rm esl}$ to the nominal eustatic contribution $\Delta\zeta^{\rm n}_{\rm esl}$ based on the above ice

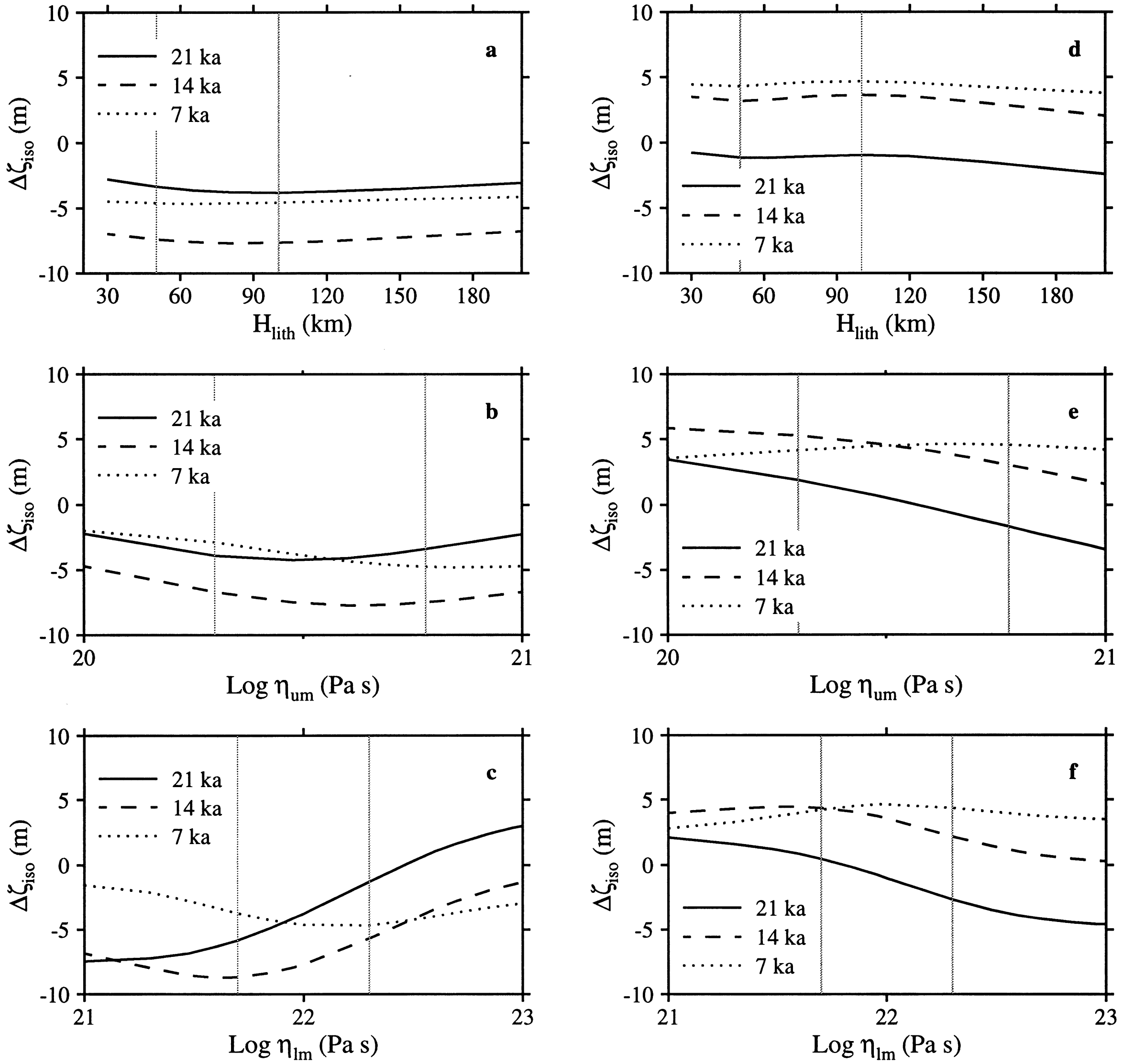

Fig. 2. Dependence of the total isostatic component $\Delta\zeta_{iso}$ of relative sea-level change on earth rheology parameters for Barbados (a, b, c) and the Huon Peninsula (d, e, f) using the nominal ice model. The vertical lines are the boundaries of the parameter ranges used to determine the rheology dependent uncertainty (Table 1). (a, d) dependence on lithosphere thickness for $\eta_{um} = 5 \times 10^{20}$ Pa s, $\eta_{lm} = 10^{22}$ Pa s, (b, e) dependence on upper mantle viscosity for $H_{lith} = 80$ km, $\eta_{lm} = 10^{22}$ Pa s, (c, f) dependence on lower mantle viscosity for $H_{lith} = 80$ km, $\eta_{um} = 5 \times 10^{20}$ Pa s.

models can be written as:

$$\delta\zeta_{esl} = \Delta\zeta_{obs}(\tau, \varphi) - (\Delta\zeta^{n}_{est} + \Delta\zeta_{iso}) \tag{3}$$

The accuracy estimates $\delta\zeta_{esl}$ are approximately $(\sigma^2_{obs} + \sigma^2_{pred})^{1/2}$ where σ_{obs} is the standard deviation of the observed values and σ_{pred} is a measure of the spread of the predicted values for the range of earth rheologies discussed above (Table 1). The observational uncertainties usually cannot be defined by known probability distributions and estimates of the lower and upper limits to the observed values are used as a measure of σ_{obs}. These limits may not be

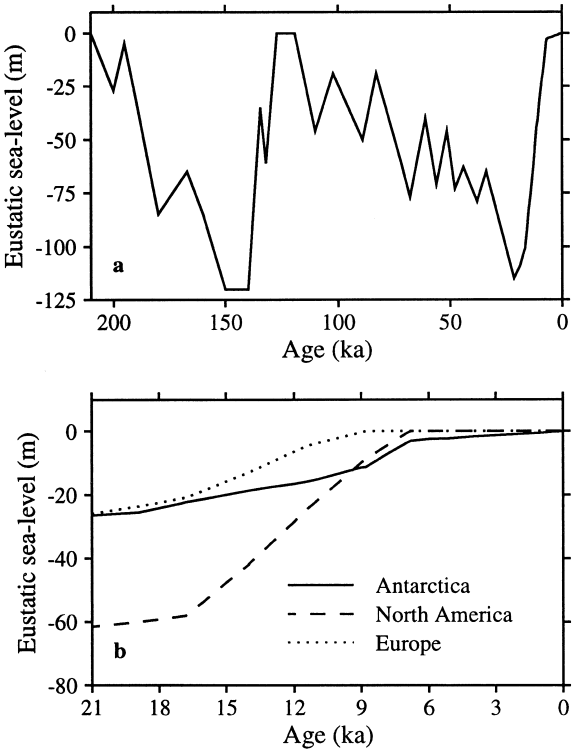

Fig. 3. (a) The eustatic curve of the nominal ice model. (b) The eustatic contributions since the Last Glacial Maximum for the three principle ice sheets.

equal, resulting in some instances in an asymmetry in the accuracy estimates of $\delta\zeta_{esl}$.

3.4. Corrections to data

Model predictions refer to mean sea level, while observations usually refer to some point in the tidal range, or represent only a limit to the position of sea level. Thus sea level estimates from freshwater peats have been corrected for the height of the highest astronomical tide and brackish water peats corrected for the height of the spring tide, but in both cases the resulting observations still only provide an upper limit. Likewise, corals have been corrected for the height of the mean-low-water spring tide but most coral observations will represent lower limits to the sea-level position. Tectonic corrections have been applied, using published rates of uplift or subsidence that usually represent average values over 10^5 years or more [16,17]. Most of the original observations used here have been dated using ^{14}C or U–Th and ages based on the former have been calibrated using the CALIB 3.0 conversion program [18,19]. For the ^{14}C ages that lie beyond the range of CALIB 3.0 a linear regression using coral samples dated by both ^{14}C and U–Th from the LGP has been used.

4. Defining the eustatic sea-level curve

4.1. The Last Glacial Maximum

Table 2 summarises the data used (Fig. 1). Those from Barbados [17,19–21] include two *Porites asteroides*, a deeper water species, and nine *Acropora palmata*, a shallow water species that is usually found to depths of 5 m although this may reach 10 m in mixed assemblages [22]. The elevation of Last Interglacial *Acropora* facies is used to estimate a mean uplift rate of 0.34 mm yr^{-1} for Barbados and all depths of the corals from this location have been corrected using this rate. The two coral observations from Mayotte (Comoro Islands, western Indian Ocean, Fig. 1) are identified as *Acropora* and *Galaxea fascicularis* taken to represent lower limits and where tectonic subsidence has been estimated as 0.19 ± 0.07 mm yr^{-1} [23,24]. The sample from Irabu Island (Ryuku, Japan) is a *Platygyra* coral [25] which lives to depths of at least 10 m, also considered here a lower limit. Two of the African data points are from offshore Cape St. Francis (South Africa), a *Pecten* and an oyster shell, dredged from presumed ancient beaches [26]. Both are taken to represent lower limits due to the likelihood of reworking [27]. The third observation is a *Porites* coral from the continental shelf around Guinea (West Africa), regarded as a lower limit as it came from a broken algal rock [28]. The three data points from the Timor Sea (Northwest Australia) are dredged *Chlamys senatorius* shells, a littoral living species, and two samples of silty clay that are indicative of lagoonal/shallow marine conditions and are interpreted as lower limits [29,30]. The observation from offshore New South Wales (Eastern Australia) is a *Pecten fumatus* shell from a vibracore (112/VC/134) near the edge of the continental margin at a depth of 150 m. This observation is also a lower limit as *P. fumatus* lives in water 10 to 50 m deep [31,32].

Table 2
Sea-level indicator data and calculated eustatic values from various sites for the Last Glacial Maximum; observed ($\Delta\zeta_{obs}$) and corrected ($\Delta\zeta_{cor}$) range of elevations. The later include the depth range of the indicator, tidal range and tectonic movement. $\Delta\zeta_{iso}$ and $\Delta\zeta_{eus}$ are the total isostatic component of sea-level change and calculated eustatic values respectively

Locality	Identification and material	Age	$\Delta\zeta_{obs}$ (m)	$\Delta\zeta_{cor}$ (m)	$\Delta\zeta_{iso}$ (m)	$\Delta\zeta_{eus}$ (m)
Barbados [17,19–21]	RGF15-10-6 (Ap)	17120 [b]	−102.0	−106.9 to −101.9	−7.3 to −2.2	−104.7 to −94.6
	RGF15-12-2 (Ap)	18530 [b]	−103.2	−108.4 to −103.4	−7.3 to −1.9	−106.5 to −96.2
	RGF13-8-9 (Ap)	17190 [b]	−106.0	−110.8 to −105.8	−7.3 to −2.2	−108.6 to −98.6
	RGF9-21-11 (Ap)	18240 [a]	−106.0	−111.2 to −106.2	−7.3 to −1.9	−109.2 to −99.0
	RGF9-23-2 (Ap)	17720 [b]	−107.3	−112.4 to −107.4	−7.3 to −2.1	−110.3 to −100.1
	RGF9-24-2 (Ap)	18020 [b]	−109.2	−114.3 to −109.3	−7.3 to −2.0	−112.3 to −102.0
	RGF9-24-4 (Ap)	18890 [a]	−109.3	−114.6 to −109.6	−7.3 to −1.8	−112.8 to −102.4
	RGF9-27-4 (Ap)	18430 [b]	−113.8	−119.1 to −114.1	−7.3 to −1.9	−117.2 to −106.9
	RGF9-27-5 (Ap)	19000 [a]	−113.8	−119.5 to −114.5	−7.2 to −1.7	−117.8 to −107.4
	RGF9-32-4 (Pa)	20610 [a]	−119.8	>−125.4	−6.5 to −0.9	>−124.6
	RGF9-34-8 (Pa)	22030 [b]	−124.4	>−130.6	−6.1 to −0.5	>−130.1
Mayotte [23,24]	BRGM-071 (Ac)	18200 [a]	−118	>−115.8	−11.0 to −6.6	>−109.2
	BRGM-079 (Gf)	18400 [a]	−152	>−149.8	−11.1 to −6.6	>−143.2
Irabu Island [25]	? (Pl)	22170 [a]	−126.2	>−126.2	−16.9 to −11.8	>−114.4
South Africa [26,27]	Pta-182 (Pec)	20090 [b]	−130	>−130	1.0 to 7.7	>−137.7
	Pta-265 (Oy)	17380 [b]	−112	>−112	2.5 to 8.5	>−120.5
Guinea [28]	I-3678 (Pb)	22600 [c]	−111 to −103	>−111	3.4 to 8.7	>−119.7
Northwest Shelf [29,30]	LJ-516 (Cs)	19980 [b]	−132	−130 to −134	−7.7 to −3.1	−130.9 to −122.3
	LJ-998 (sc)	20690 [b]	−133	>−133	0.0 to 5.3	>−138.3
	LJ-999 (sc)	22790 [c]	−134	>−134	−0.7 to 4.6	>−138.6
Offshore NSW [31,32]	SUA-3050 (Pf)	20570 [b]	−150.6	>−150.6	2.1 to 6.7	>−157.3

[a] U–Th date, [b] mean calibrated ^{14}C date, [c] calibrated ^{14}C date using a linear regression.
Ac *Acropora*, sp., Ap *Acropora palmata*, Gf *Galaxea fascicularis*, Pa *Porites asteroides*, Pb *Porites bernardi*, Pf *Pecten fumatus*, Pec *Pecten sp*., Oy oyster, Pl *Platygyra* sp., Cs *Chlamys senatorius*, sc silty clay.

Table 2 summarises these LGM observations together with their estimated upper and lower limits of sea level. Also shown is the isostatic correction for each locality, based on the range of earth-models from Table 1. The final column gives the upper and lower estimates for the eustatic sea levels corresponding to each observation. These are illustrated in Fig. 4 together with the nominal eustatic function for the LGM interval. Within the uncertainties of individual estimates, including both the observational limits and the range of plausible isostatic corrections, the nominal eustatic function provides a reasonable representation for the period from 17 to 23 ka, although its accuracy remains relatively low. The Barbados corals dated between 17 and 19 ka indicates that the eustatic level estimate may be too large (ca. 10 m) for this interval whereas the data points between about 20 and 21 ka indicate that the maximum eustatic level may have been lower during an early stage of the LGM with the maximum value occurring between 120 and 130 m below present mean sea level. In terms of ice volume, this equates to (4.6–4.9) $\times 10^7$ km^3 of land-based ice in excess of what is present today.

4.2. Late Glacial Period

The LGP data are from Barbados, the Huon Peninsula and Tahiti (Fig. 1). The Barbados observations [17,19–21] include those used to define the LGM levels. The Huon Peninsula observations are from a 52 m core drilled through continuous coral framework [33,34]. Corrections for tectonic uplift at a rate of 1.9 mm yr^{-1} [33] have been applied. This rate appears to have been uniform over long periods of time (10^4 to 10^5 years) although there is evidence for metre scale coseismic events [35]. The Tahiti data is from two cores drilled through the Papeete outer reef and comprises different corals that grew on a high-energy reef-front in 5–15 m of water [36,37].

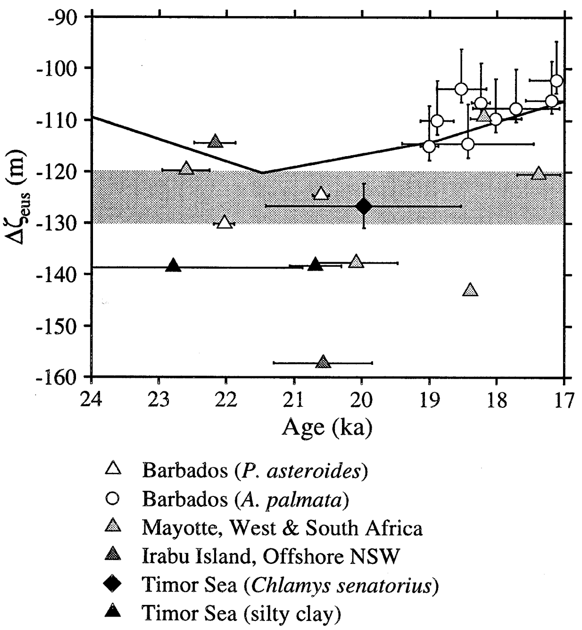

Fig. 4. Eustatic values derived from observations for the Last Glacial Period (LGM). The solid line represents the nominal eustatic curve. Triangles represent lower limit estimates. The shaded area represents the proposed range for the LGM eustatic sea level. Age uncertainties in this and subsequent figures correspond to 2σ estimates.

The reef itself is believed to be subsiding at a rate of 0.2 mm yr^{-1} [36].

Fig. 5 presents the observations for the three sites, including corrections for tectonic movement where appropriate, together with the range of predicted changes based on the nominal eustatic sea-level model and the range plausible rheologies (Table 1). Since all data points correspond to in situ corals, the actual sea level curves lies above the observed values by as much as 5–15 m. Agreement between observations and predictions of relative sea level is generally satisfactory, with the later mostly lying above the observations. However, at both the Huon Peninsula and Tahiti, this difference attains about 15 m, and particularly at the later site the offset is systematic for the entire period. It has been suggested that the upper mantle viscosity beneath the Society Islands may be anomalously low [38] and less than the lower limit considered in the model range explored, but this only shifts the predicted sea levels to shallower values and increase the offset. Possibly the high-energy reef front of this site means that only deeper corals have been well preserved.

The inferred eustatic values $(\Delta\zeta^{\mathrm{n}}_{\mathrm{est}} + \delta\zeta_{\mathrm{esl}})$ are also illustrated in Fig. 5 for the three localities, along with the nominal function $\Delta\zeta^{n}_{est}$. For Barbados, the corrective terms $\delta\zeta_{\mathrm{esl}}$ are generally small, with the possible exception that near 14 ka the rapid rise already noted in [17] is not reproduced by the nominal model $\Delta\zeta^{\mathrm{n}}_{\mathrm{esl}}$. The records from the other two localities do not extend sufficiently far back in time to verify this change and the possibility remains that is a sampling artefact, particularly as it occurs in a break between two cores ([39], RGF-12 and RGF-9). It has also been suggested [40] that the Barbados record points to a second period of rapid sea level rise, between about 11.6 and 11.1 ka. This is also at a break between cores (RGF-7 and RGF-12), and is not seen in the records from the other two localities. The rise of sea level seen in the Huon Peninsula record is slower than average between about 12 and 11 ka, however the Barbados record contains only three points between 10.1 and 12.3 ka.

4.3. Post Glacial Period

The observations from the PGP, shown in Fig. 6 together with the predicted upper and lower limits, are from the Great Barrier Reef (GBR), the Senegal River (West Africa), Jamaica and the west coast of Malaysia (Fig. 1). The Great Barrier Reef observations consist of the ages and heights above present-day growth positions of coral (predominantly *Porites* Sp.) microatolls [12,41]. The observations from the Senegal River consist of marine molluscs and inter-tidal (mangrove) peats [42]. The Jamaica data set consists of various peat samples (transition, sedge, mangrove, swamp forest) from two wetland areas situated on Tertiary limestone platforms [43]. Only basal samples resting on or near the limestone bedrock or on late-Pliocene to Pleistocene clays have been used in order to minimise the effects of compaction of both the peat and underlying sediments. The west coast of Malaysia data consists of various organic materials (peat, wood, shells), collected from onshore and offshore [44–47] and whose relationships to mean sea level are not always obvious. Compaction may have occurred for the peat samples [45].

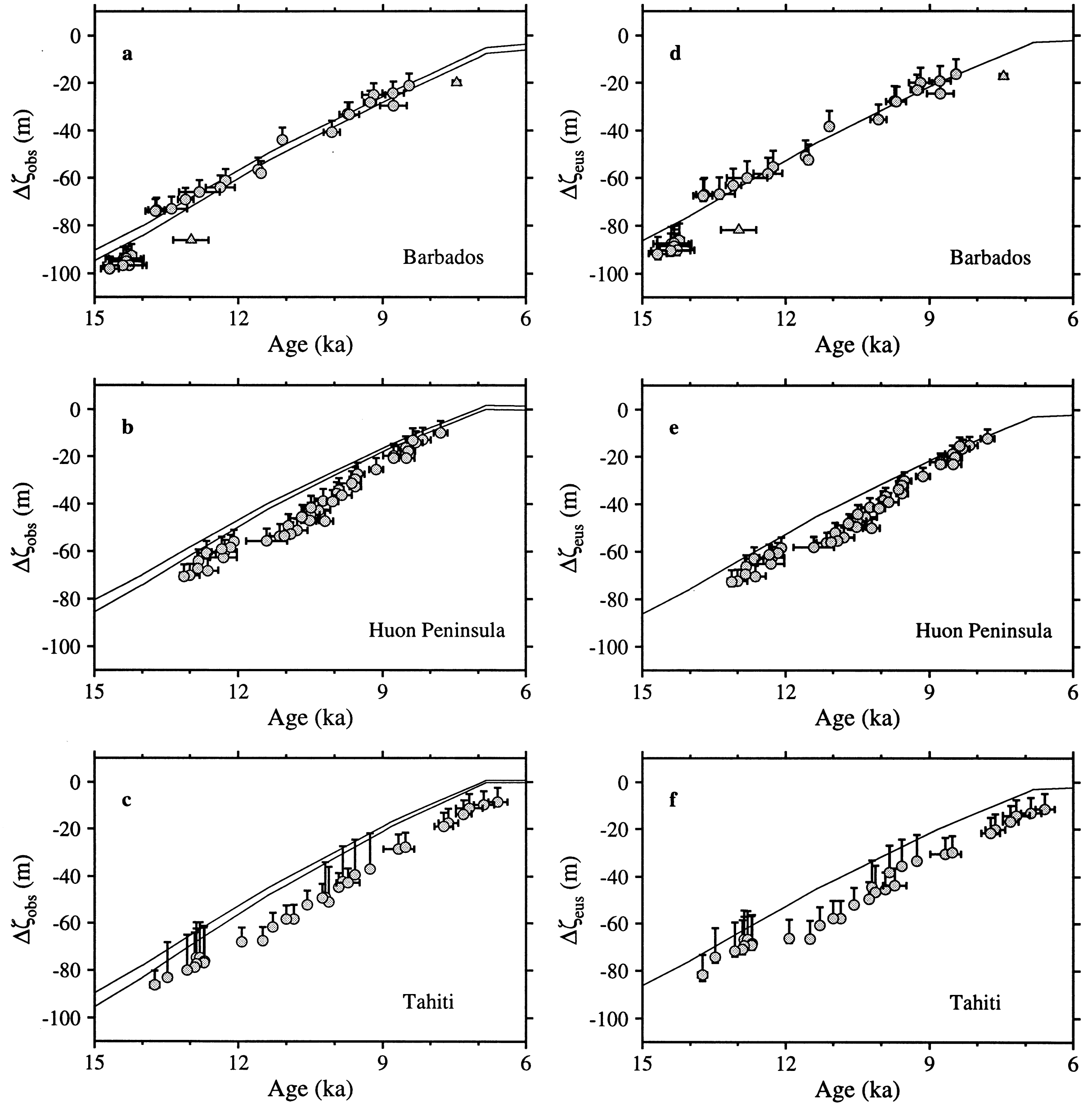

Fig. 5. Observations (a, b, c) and estimated eustatic values (d, e, f) from the Late Glacial Period sites. The solid lines in (a, b, c) represent the maximum and minimum modelled limits of relative sea-level change based on the range of rheologies in Table 1. The solid line in (d, e, f) represents the nominal eustatic curve. The observational data has been adjusted for uplift/subsidence. The height error bars on observations indicate the depth ranges of the sea-level indicators, while those on eustatic values are the combined depth range and earth rheology uncertainty.

The predictions for the GBR, Senegal, and Malaysia, with the development of highstands at about 7 ka, are characteristic of far-field continental margins localities, with the amplitudes of the highstand depending on shoreline geometry. The Malaysian highstand is particularly well developed

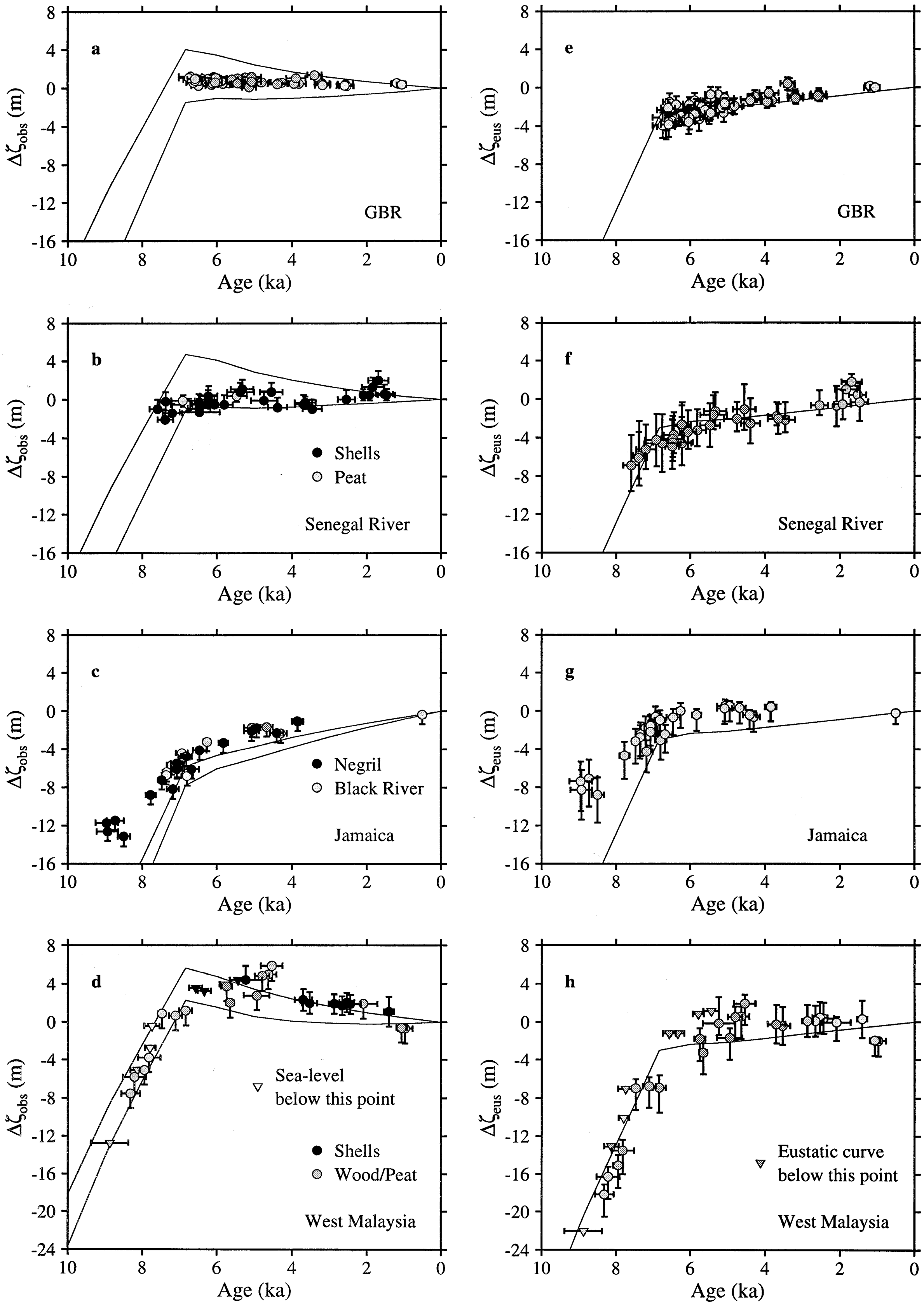
a
GBR
e
GBR
b
Shells
Peat
Senegal River
f
Senegal River
c
Negril
Black River
Jamaica
g
Jamaica
d
Sea-level
below this point
Shells
Wood/Peat
West Malaysia
h
Eustatic curve
below this point
West Malaysia
Δζobs (m)
Δζeus (m)
Age (ka)

because of the response of the lithosphere and upper mantle to the flooding of the Malacca Straits during the deglaciation phase. In contrast, the Jamaica predictions are characteristic of intermediate-field sites where the glacio-isostatic contribution dominates the hydro-isostatic part. For all areas except Jamaica (Fig. 6g), the observations lie, for the most part, within the limits of the predictions based on the rheology range (Table 1). Of these sites, Jamaica is also the most sensitive to details of the nearby Laurentide ice sheets.

Fig. 6 also presents the inferred eustatic values ($\Delta\zeta^{n}_{esl} + \delta\zeta_{esl}$) with the nominal eustatic model. The GBR predictions are in good agreement with this nominal model, in part because a subset of this data was used, amongst other data, to derive the eustatic function [12]. The predictions tend to lie marginally below the nominal function between about 7 and 6 ka and above it for the more recent period. Otherwise, scatter about this function is minimal and any short-duration oscillations in ocean volume are likely to have been small over this period, consistent with earlier inferences [48]. The Senegal River results (Fig. 6f) show a similar form between 7 and 6 ka, although the deviation is greater. Estimates between 8 and 7 ka tend to be above the nominal curve, a trend that has been noted in analyses from some other localities [49]. The Jamaica results (Fig. 6g) exhibit a greater discrepancy for this early period lying above the nominal values throughout the interval by as much as 9 to 14 m. The results from Malaysia, while more scattered, are in good agreement with the nominal eustatic model, particularly in the interval between 9 and 6 ka.

5. Discussion

Fig. 7 presents all of the eustatic sea-level estimates for the period between the LGM and end of the LGP (Fig. 7a), the eustatic residuals $\delta\zeta_{esl}$ for the same period (Fig. 7b), the eustatic estimates for the PGP (Fig. 7c) and the associated residuals (Fig. 7d). Note that some overlap in time occurs between the two data groups. As previously noted, for the LGM interval, the residuals in the interval 22 to 20 ka are primarily negative, suggesting that the ice volumes at that time were greater than assumed in the nominal eustatic model, with the reverse occurring between 19 and 17 ka. Thus the evidence points to maximum ice volumes having occurred at around 22–20 ka (ca. 19–17 ka ^{14}C ka) and that from this time to about 17 ka enough land-based ice had melted to raise the eustatic sea level by between 20 and 30 m, an average rate of ca. 6 m ka^{-1}, equivalent to ca. (8–12) $\times$ 10^{6} km^{3} of land-based ice. A critical gap occurs in the data between 17 and 15 ka. At about 15–14 ka the Barbados data indicates that the eustatic level may have been a few metres lower than assumed by the nominal model. Thus a tentative inference is that during the interval 19 to 15 ka, eustatic levels rose uniformly but at a rate less than in the nominal model (see dotted line in Fig. 8a).

At about 14 ka the Barbados data points to a rapid sea-level rise, in less than 500 years, of about 7–8 m in excess of the nominal rate of sea-level change (ca. 5 m) *if* it can be assumed that the growth rates of the corals were equal to the sea level rise at a time when ice sheet decay became rapid but ocean temperatures were still relatively cold. That the observations before and after this time correspond to different coral colonies serves as a further caution in the interpretation. For the latter part of the LGP a comparison of results between the three localities is possible. The Huon Peninsula and Tahiti residuals generally lie below those for Barbados, the offset in the interval 14–12 ka being of the order 7–8 m (Fig. 7b), this further emphasises the need for caution in the interpretation of single coral core records. Possibly the explanation lies in different growth depths for the corals sampled, in rates of tectonic subsidence or uplift not being constant, or in a lateral variation

Fig. 6. Observations (a, b, c, d) and estimated eustatic values (e, f, g, h) from the Post Glacial Period sites. The solid lines in (a, b, c, d) represent the maximum and minimum modelled limits of relative sea-level change based on the range of rheologies in Table 1. The solid line in (e, f, g, h) represents the nominal eustatic curve. The observational data has been adjusted for uplift/subsidence. The height error bars on observations indicate the depth ranges of the sea-level indicators, while those on eustatic values are the combined depth range and earth rheology uncertainty.

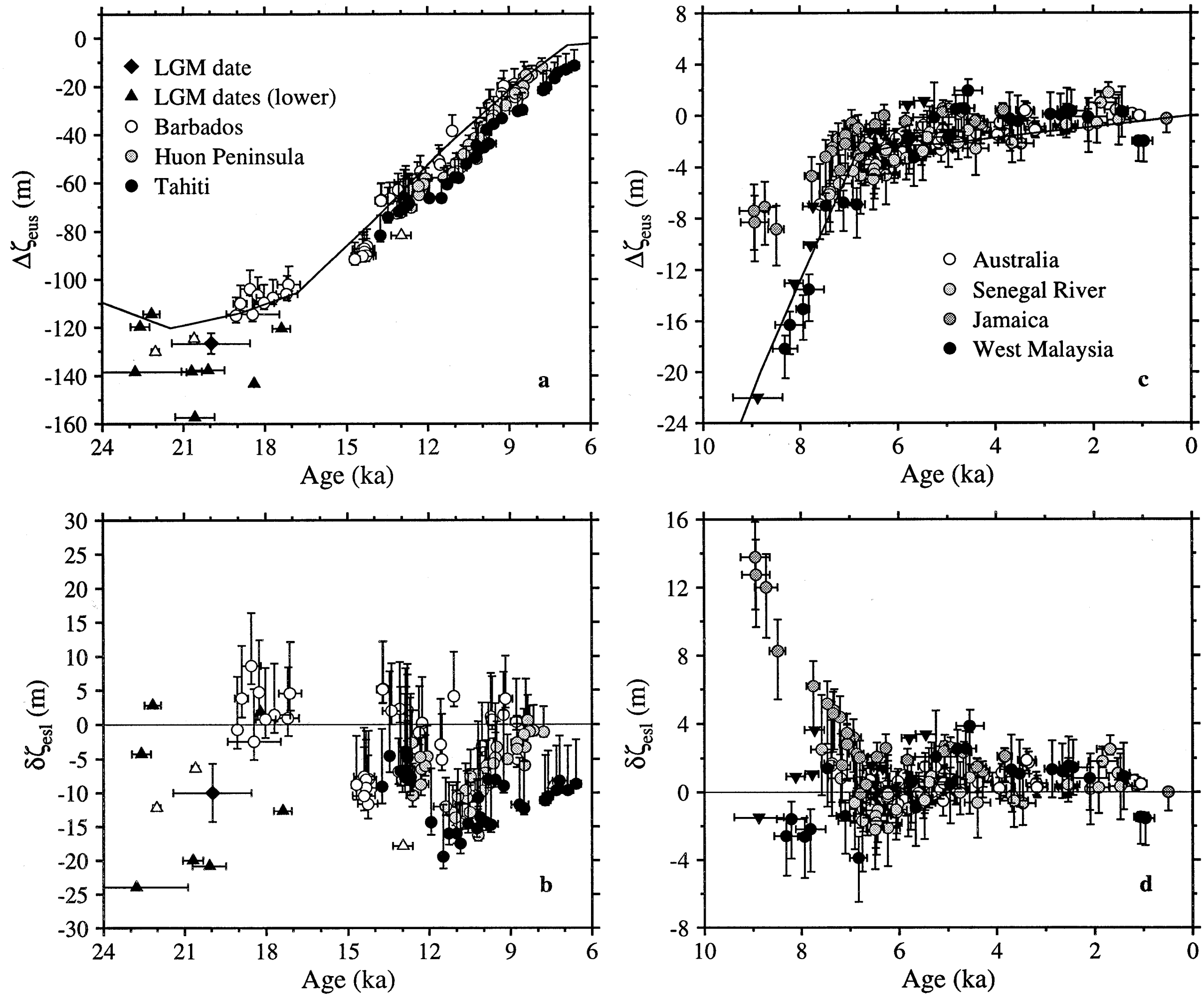

Fig. 7. (a) The estimated eustatic sea-level change for the combined data set spanning the Last Glacial Maximum to the Late Glacial Period; (b) the corresponding eustatic residuals defined by Eq. 3; (c, d) the same as (a, b) but for the Post Glacial Period.

in mantle parameters that lie outside the limits imposed in the isostatic correction calculation. Within the interval 15–8 ka the residuals (Fig. 7b) do appear to exhibit some pattern, the structure of which follows in part the results for the individual cores. For example, both the Huon Peninsula and Tahiti data from about 12 to 9 ka indicate that the eustatic rise may have been more rapid than assumed if the single Barbados result at 11.1 ka is ignored.

The eustatic estimates for the latter part of the Holocene (Fig. 7c, 7d), from about 7 ka to the present, show a consistent pattern in which the residuals are generally positive after about 6 ka. At the end of the major phase of deglaciation of the northern ice sheets, at about 7 ka eustatic sea level was ca. 3–5 m below the present level. This is consistent with earlier conclusions based on local data sets [8,49,50] and indicates that minor deglacia-

Fig. 8. The combined estimated eustatic sea-level results (a) from the Last Glacial Maximum to the present day, and (b) for the Holocene. The initial nominal eustatic curve $\Delta\zeta^{n}_{esl}$ (solid) and a modified eustatic curve $\Delta\zeta^{m}_{esl}$ (dotted) are also shown.

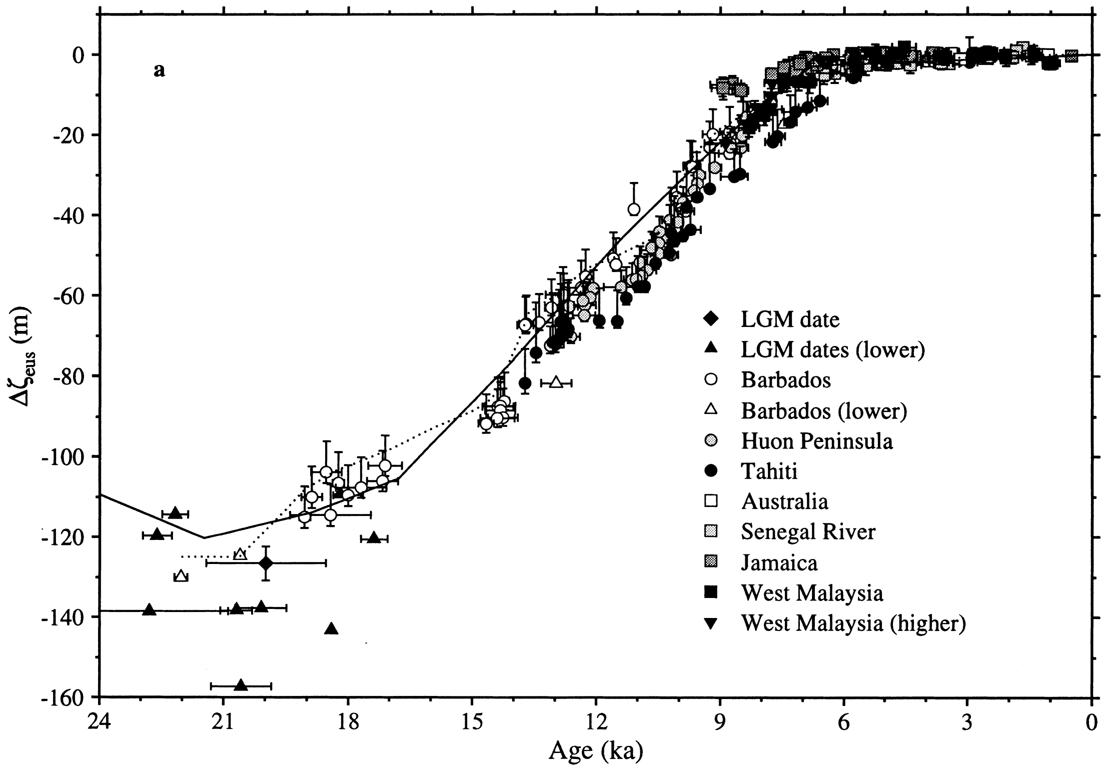
a
0
-20
-40
-60
-80
-100
-120
-140
-160
Δζeus (m)
24
21
18
15
12
9
6
3
0
Age (ka)
LGM date
LGM dates (lower)
Barbados
Barbados (lower)
Huon Peninsula
Tahiti
Australia
Senegal River
Jamaica
West Malaysia
West Malaysia (higher)

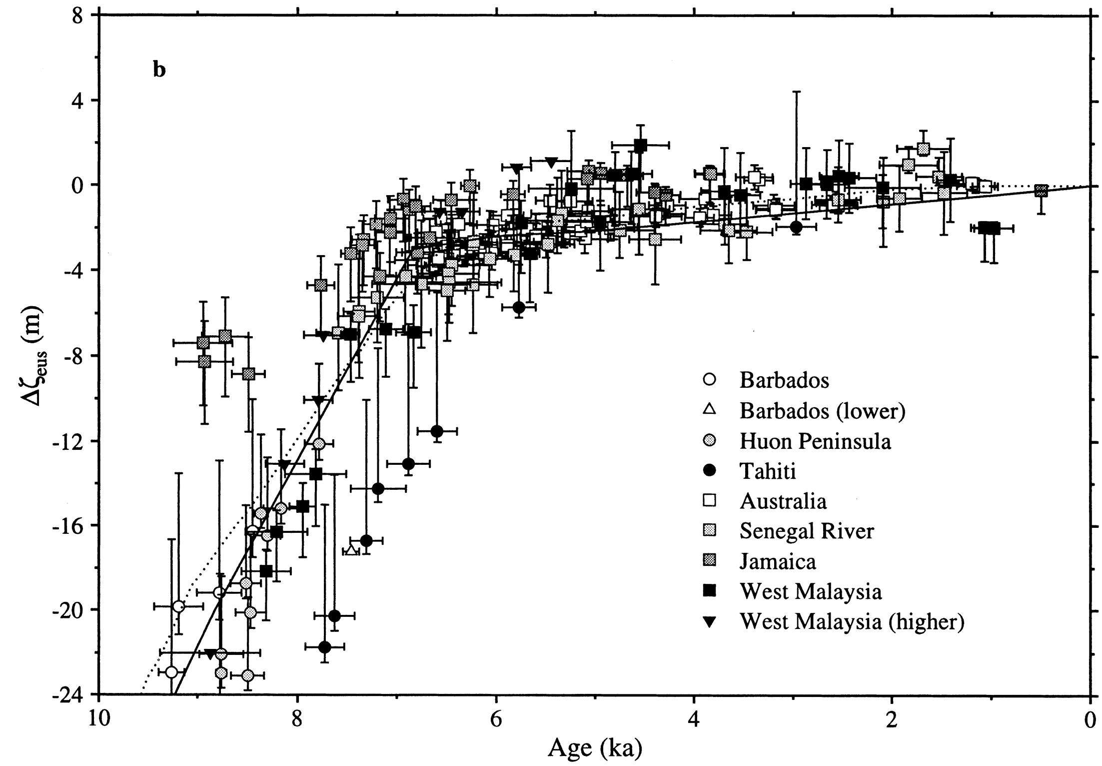
b
8
4
0
-4
-8
-12
-16
-20
-24
Δζeus (m)
10
8
6
4
2
0
Age (ka)
Barbados
Barbados (lower)
Huon Peninsula
Tahiti
Australia
Senegal River
Jamaica
West Malaysia
West Malaysia (higher)

tion, possibly from Antarctica or temperate mountain glaciers, continued into Late-Holocene times, until about 2–1 ka according to the residuals in Fig. 7d. Considerable scatter occurs in the residuals for the past 7000 years but no consistent pattern with it appearing to be primarily associated with local factors: for example (i) the development of moats on the developing GBR reef flats leads to a growth limit of microatolls that exceeds the assumed mean low water spring level [48]; (ii) fluctuations in coastline geometry through time can result tidal ranges different from the assumed values based on present day tides; (iii) local tectonics, compaction and consolidation. The absence of significant oscillations in sea level during this interval is consistent with the results of detailed analyses from locally restricted areas in, for example, Queensland, Australia [48] and the French Atlantic coast [49]. Between 9 and 7 ka a major anomaly occurs for the Jamaica data points which are consistently high when compared with the Malacca Straits data or with the coral data for the same period. The answer to this may lie in the interpretation of the observational record, in erroneous age determination for the material, in local tectonics [43], or in inadequacies in the adopted model for the Laurentide ice sheet.

Fig. 8 combines the LGM, LGP and PGP derived eustatic results along with a modified eustatic curve $\Delta\zeta^{m}_{esl}$ that shows minimal variation in the rates of sea-level change but which is consistent with much of the data. With this interpretation, the majority of corals in the LGP would have been located in water depth between 0 and 10 m (Fig. 9), consistent with the growth range of most of the species used. As previously noted, periods of accelerated sea-level rise such as at 14 ka are based on a few records only and must be treated with caution. Possibly more significant is the reduced rate of sea-level rise between 12 and 11 ka which corresponds to the Younger Dryas cold period when ice sheet margins may have been stationary for a period of time. The data record of this interval is, however, also sparse and additional records from other localities are desirable.

Fig. 10 presents the total volume of ice which had accumulated and decayed, in excess of what is present today as determined by the new nominal curve presented in Fig. 8. What this result does not do is determine how that ice was distributed between the major and minor ice sheets (as well as other areas not included such as mountain glaciers) and this can only be resolved from more detailed isostatic studies around each of the regions of former glaciation (e.g. [11,12]).

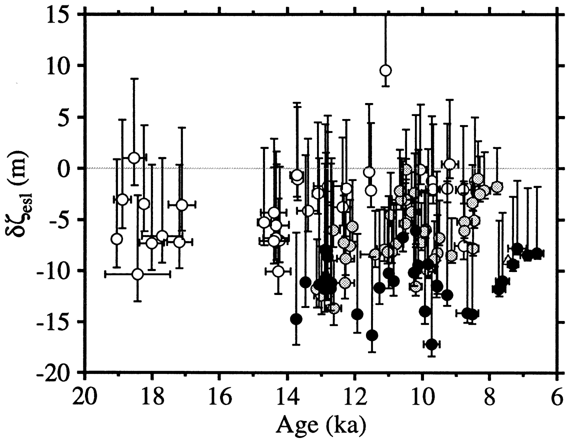

Fig. 9. Discrepancies between the observed and predicted sea-levels for the combined Late Glacial Period data set with the predictions based on the modified eustatic sea-level curve.

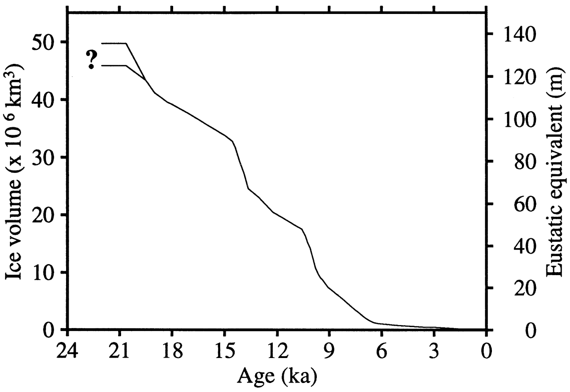

Fig. 10. The equivalent ice volumes which would have been required to produce the modified eustatic sea-level curve. The question mark indicates the uncertainty involved in the ice volumes during the Last Glacial Maximum.

6. Conclusion

The eustatic sea-level function since the LGM can be characterised by three principal features: (1) a minimum level of ca. 125 ± 5 m at the time of the

LGM, (2) a nearly uniform rise from around 15 ka to 7 ka of ca. 10 m ka^{-1} and (3) a constant value for the last 7000 years. Some departures from this simple function, however, occur. In decreasing order of confidence, these are: (1) ocean volumes continued to increase during the late Holocene (PGP) period, rising by 3–5 m over the period 7 ka to the present day, with most melting finally completed by 2–1 ka, consistent with conclusions drawn earlier [8,49,50]; (2) no significant high frequency oscillations in global sea levels have occurred in the past 7000 years; (3) rates of increase in ocean volumes for the early LGP from 19 to 15 ka are generally lower than for the later part of this phase; (4) the maximum glaciation may have occurred between 22–20 ka, with an initial period of deglaciation occurring at about 20–18 ka; (5) fluctuations in the rate of sea-level rise for the LGP may have occurred at two periods, at the time of the Younger Dryas and again at about 14 ka, but for neither is the current evidence compulsive. ***[AC]***

References

[1] K. Lambeck, Glacial rebound and sea-level change: an example of a relationship between mantle and surface processes, Tectonophysics 223 (1993) 15–37.

[2] J. Chappell, Geology of coral terraces, Huon Peninsula, New Guinea: A study of Quaternary tectonic movements and sea-level changes, Geol. Soc. Am. Bull. 85 (1974) 553–570.

[3] W.E. Farrell, J.A. Clark, On postglacial sea level, Geophys. J. R. Astron. Soc. 46 (1976) 647–667.

[4] J.A. Clark, W.E. Farrell, W.R. Peltier, Global changes in postglacial sea level: a numerical calculation, Quat. Res. 9 (1978) 265–298.

[5] J.X. Mitrovica, W.R. Peltier, On postglacial geoid subsidence over the equatorial oceans, J. Geophys. Res. 96 (1991) 20053–20071.

[6] P. Johnston, The effect of spatially non-uniform water loads on prediction of sea-level change, Geophys. J. Int. 114 (1993) 615–634.

[7] G.A. Milne, J.X. Mitrovica, Postglacial sea-level change on a rotating Earth: first results from a gravitationally self-consistent sea-level equation, Geophys. J. Int. 126 (1996) F13–F20.

[8] M. Nakada, K. Lambeck, The melting history of the Late Pleistocene Antarctic ice sheet, Nature 333 (1988) 36–40.

[9] A.M. Dziewonski, D.L. Anderson, Preliminary reference Earth model, Phys. Earth Planet. Inter. 25 (1981) 297–356.

[10] J.X. Mitrovica, W.R. Peltier, The inference of mantle viscosity from an inversion of the Fennoscandian relaxation spectrum, Geophys. J. Int. 114 (1993) 45–62.

[11] K. Lambeck, C. Smither, P. Johnston, Sea-level change, glacial rebound and mantle viscosity for northern Europe, Geophys. J. Int. 134 (1998) 102–144.

[12] D. Zwartz, The recent history of the Antarctic Ice Sheet: Constraints from sea-level change, Ph.D. Thesis, The Australian National University, 1995.

[13] M. Nakada, K. Lambeck, Glacial rebound and relative sealevel variations: A new appraisal, Geophys. J. R. Astron. Soc. 90 (1987) 171–224.

[14] W.R. Peltier, J.T. Andrews, Glacial-isostatic adjustment: I. The forward problem, Geophys. J. R. Astron. Soc. 46 (1976) 605–646.

[15] N.J. Shackleton, Oxygen isotopes, ice volume and sea level, Quat. Sci. Rev. 6 (1987) 183–190.

[16] J. Chappell, A. Omura, T. Esat, M. McCulloch, J. Pandolfi, Y. Ota, B. Pilans, Reconciliation of late Quaternary sea levels derived from coral terraces at Huon Peninsula with deep sea oxygen isotope records, Earth Planet. Sci. Lett. 141 (1996) 227–236.

[17] R.G. Fairbanks, A 17,000-year glacio-eustatic sea level record: influence of glacial melting dates on the Younger Dryas event and deep ocean circulation, Nature 342 (1989) 637–642.

[18] M. Stuiver, P.J. Reimer, Extended ^{14}C data base and revised CALIB 3.0 age calibration program, Radiocarbon 35 (1993) 215–230.

[19] E. Bard, M. Arnold, R.G. Fairbanks, B. Hamelin, ^{230}Th–^{234}U and ^{14}C ages obtained by mass spectrometry on corals, Radiocarbon 35 (1993) 191–199.

[20] E. Bard, B. Hamelin, R.G. Fairbanks, A. Zindler, Calibration of the ^{14}C timescale over the past 30,000 years using mass spectrometric U–Th ages from Barbados corals, Nature 345 (1990) 405–410.

[21] E. Bard, B. Hamelin, R.G. Fairbanks, U–Th ages obtained by mass spectrometry in corals from Barbados: sea level during the past 130,000 years, Nature 346 (1990) 456–458.

[22] R.G. Lighty, I.G. Macintyre, R. Stuckenrath, *Acropora Palmata* reef framework: A reliable indicator of sea level in the Western Atlantic for the past 10,000 years, Coral Reefs 1 (1982) 125–130.

[23] M. Colonna, J. Casanova, W.-C. Dullo, G. Camoin, Sea-level changes and $d^{18}O$ record for the past 34,000 yr from Mayotte Reef, Indian Ocean, Quat. Res. 46 (1996) 335–339.

[24] W.-C. Dullo, G. Camoin, D. Blomeier, M. Colonna, A. Eisenhauer, G. Faure, J. Casanova, B.A. Thomassin, Morphology and sediments of the foreslopes of Mayotte, Comoro Islands: Direct observations from submersibles, in: G. Camoin, D. Bergerson (Eds.), Reefs and Carbonate Platforms of the Indian Ocean and the Pacific, IAS Spec. Pub. (in press)

[25] A. Omura, K. Sasaki, T. Miwa, Y. Isuji, H. Matsuda, T. Nakamori, Y. Iryu, T. Yamada, Y. Sato, H. Nakagawa, Radiometric dates of carbonate sediments beneath the edge of insular shelf off Irabu Island, southwestern Ryukyus, Japan, in: Annual Meeting of Japan Association for Quaternary Research, 1996, pp. 54–55, (in Japanese).

[26] J.C. Vogel, M. Marais, Pretoria radiocarbon dates I, Radiocarbon 13 (2) (1971) 378–394.
[27] D.E. Miller, A Southern African late Quaternary sea-level curve, S. Afr. J. Sci. 86 (1990) 456–458.
[28] R.L. McMaster, T.P. Lachance, A. Ashraf, Continental shelf geomorphic features off Portuguese Guinea, Guinea, and Sierra Leone (West Africa), Mar. Geol. 9 (1970) 203–213.
[29] T.H. van Andel, J.J. Veevers, Morphology and sediments of the Timor Sea, BMR J. Aust. Geol. Geophys. 82 (1967) 1–73.
[30] T. van Andel, G. Ross Heath, T.C. Moore, D.F.R. McGeary, Late Quaternary history, climate and oceanography of the Timor Sea, Northwestern Australia, Am. J. Sci. 265 (1967) 737–758.
[31] M.A. Ferland, P.S. Roy, C.V. Murray-Wallace, Glacial lowstand deposits on the outer continental shelf of southeastern Australia, Quat. Res. 44 (1995) 294–299.
[32] C.V. Murray-Wallace, M.A. Ferland, P.S. Roy, A. Sollar, Unravelling patterns of reworking in lowstand shelf deposits using amino acid racemisation and radiocarbon dating, Quat. Sci. Rev. 15 (1996) 685–697.
[33] J. Chappell, H. Polach, Post-glacial sea-level rise from a coral record at Huon Peninsula, Papua New Guinea, Nature 349 (1991) 147–149.
[34] R.L. Edwards, J.W. Beck, G.S. Burr, D.J. Donahue, J.M.A. Chappell, A.L. Bloom, E.R.M. Druffel, F.W. Taylor, A large drop in atmospheric $^{14}C/^{12}C$ and reduced melting in the Younger Dryas, documented with ^{230}Th ages of corals, Science 260 (1993) 962–968.
[35] J. Chappell, Y. Ota, K. Berryman, Late Quaternary coseismic uplift history of Huon Peninsula, Papua New Guinea, Quat. Sci. Rev. 15 (1996) 7–22.
[36] E. Bard, B. Hamelin, M. Arnold, L. Montaggioni, G. Cabioch, G. Faure, F. Rougerie, Deglacial sea-level record from Tahiti coral and the timing of global meltwater discharge, Nature 382 (1996) 241–244.
[37] L.F. Montaggioni, G. Cabioch, G.F. Camoinau, E. Bard, A. Ribaud-Laurenti, G. Faure, P. Déjardin, J. Récy, Continuous record of reef growth over the past 14 k.y. on the mid-Pacific island of Tahiti, Geology 25 (1997) 555–558.
[38] M. Nakada, K. Lambeck, Late Pleistocene and Holocene sea-level change: Evidence for lateral mantle viscosity structure, in: R. Sabadini, K. Lambeck, E. Boschi (Eds.), Glacial Isostasy, Sea-level and Mantle Rheology, Kluwer, Dordrecht, 1990, pp. 79–94.
[39] W.S. Broecker, Salinity history of the northern Atlantic during the last deglaciation, Paleoceanography 5 (1990) 459–467.
[40] P. Blanchon, J. Shaw, Reef drowning during the last deglaciation: Evidence for catastrophic sea-level rise and ice-sheet collapse, Geology 23 (1995) 4–8.
[41] J. Chappell, A. Chivas, E. Wallensky, H.A. Polach, P. Aharon, Holocene palaeo-environmental changes, Central to North Great Barrier Reef inner zone, BMR J. Aust. Geol. Geophys. 8 (1983) 223–235.
[42] H. Faure, J.C. Fontes, L. Hebrard, J. Monteillet, P.A. Pirazzoli, Geoidal change and shore-level tilt along Holocene estuaries: Senegal River area, West Africa, Science 210 (1980) 421–423.
[43] G. Digerfeldt, M.D. Hendry, An 8000 year Holocene sea-level record from Jamaica: implications for interpretation of Caribbean reef and coastal history, Coral Reefs 5 (1987) 165–169.
[44] M.A. Geyh, H.-R. Kudrass, H. Streif, Sea-level changes during the late Pleistocene and Holocene in the Strait of Malacca, Nature 278 (1979) 441–443.
[45] H. Streif, Holocene sea level changes in the Strait of Malacca, in: 1978 Int. Symp. on Coastal Evolution in the Quaternary, 1979, pp. 552–572.
[46] T. Yoshikawa, Inventory of Quaternary Shorelines, NODAI Research Institute, Tokyo University of Agriculture, Tokyo, Japan, 1987, 130 pp.
[47] H.D. Tjia, Sea-level changes in the tectonically stable Malay–Thai peninsula, Quat. Int. 31 (1996) 95–101.
[48] J. Chappell, Evidence for smoothly falling sea level relative to north Queensland, Australia, during the past 6,000 yr, Nature 302 (1983) 406–408.
[49] K. Lambeck, Sea-level change along the French Atlantic and Channel coasts since the time of the Last Glacial Maximum, Palaeogeogr. Palaeoclimatol. Palaeoecol. 129 (1997) 1–22.
[50] K. Lambeck, On the choice of time scale in glacial rebound modelling: mantle viscosity estimates and the radiocarbon time scale, Geophys. J. Int. 134 (1998) 647–651.